



Published in final edited form as:

Science. 2019 November 08; 366(6466): 708–714. doi:10.1126/science.aay6826.

Ancient Rome: A genetic crossroads of Europe and the Mediterranean

Margaret L. Antonio^{1,*}, Ziyue Gao^{2,3,*}, Hannah M. Moots^{4,*}, Michaela Lucci⁵, Francesca Candilio^{6,7}, Susanna Sawyer⁸, Victoria Oberreiter⁸, Diego Calderon¹, Katharina Devitofranceschi⁸, Rachael C. Aikens¹, Serena Aneli⁹, Fulvio Bartoli¹⁰, Alessandro Bedini¹¹, Olivia Cheronet⁸, Daniel J. Cotter³, Daniel M. Fernandes^{8,12}, Gabriella Gasperetti¹³, Renata Grifoni¹⁴, Alessandro Guidi¹⁵, Francesco La Pastina⁷, Ersilia Loreti¹⁶, Daniele Manacorda¹⁷, Giuseppe Matullo⁹, Simona Morretta¹⁸, Alessia Nava^{5,19}, Vincenzo Fiocchi Nicolai²⁰, Federico Nomi¹⁵, Carlo Pavolini²¹, Massimo Pentiricci¹⁶, Philippe Pergola²², Marina Piranomonte²³, Ryan Schmidt²⁴, Giandomenico Spinola²⁵, Alessandra Sperduti^{19,26}, Mauro Rubini^{27,28}, Luca Bondioli¹⁹, Alfredo Coppa^{7,†}, Ron Pinhasi^{8,†,‡}, Jonathan K. Pritchard^{2,3,29,†,‡}

¹Program in Biomedical Informatics, Stanford University, Stanford, CA, USA. ²Howard Hughes Medical Institute, Stanford University, Stanford, CA, USA. ³Department of Genetics, Stanford University, Stanford, CA, USA. ⁴Stanford University, Department of Anthropology, Stanford, CA, USA. ⁵DANTE Laboratory for the study of Diet and Ancient Technology, Sapienza Università di Roma, Rome, Italy. ⁶School of Archaeology, University College Dublin, Dublin, Ireland. ⁷Dipartimento di Biologia Ambientale, Sapienza Università di Roma, Rome, Italy. ⁸Department of Evolutionary Anthropology, University of Vienna, Vienna, Austria. ⁹Dipartimento di Scienze Mediche, Università di Torino, Torino, Italy. ¹⁰Dipartimento di Biologia, Università di Pisa, Pisa, Italy. ¹¹Ministero dei Beni e delle Attività Culturali (retired), Rome, Italy. ¹²CIAS, Department of Life Sciences, University of Coimbra, Coimbra, Portugal. ¹³Soprintendenza Archeologia, belle arti e paesaggio per le province di Sassari e Nuoro, Sassari, Italy. ¹⁴Dipartimento di Civiltà e Forme del Sapere, Università di Pisa, Pisa, Italy. ¹⁵Dipartimento di Studi Umanistici, Università degli Studi di Roma Tre, Rome, Italy. ¹⁶Curatore beni culturali presso la Soprintendenza Capitolina, Rome, Italy.

[†]Corresponding author. pritch@stanford.edu (J.K.P.); ron.pinhasi@univie.ac.at (R.P.); alfredo.coppa@uniroma1.it (A.C.).

Author contributions: R.P., J.K.P., and A.C. designed and supervised the study; H.M.M., F.C., M.L., S.S., V.O., K.D., D.M.F., R.S., and R.P. performed and supervised laboratory work; A.C., M.L., F.L.P., M.R., L.B., and A.S. designed collection strategy for archaeological material; A.C., M.L., F.C., A.S., L.B., M.R., A.N., F.L.P., F.B., A.B., G.G., R.G., A.G., E.L., D.M., S.M., V.F.N., F.N., C.P., M.Pe., P.P., M.Pi., and G.S. assembled archaeological material and advised on historical background and interpretation; G.M. and S.A. generated data for modern Italians; M.L.A., Z.G., H.M.M., D.C., R.C.A., and D.J.C. curated and analyzed data with input from D.M.F., R.P., J.K.P., and S.A.; H.M.M., M.L.A., Z.G., J.K.P., and R.P. wrote the manuscript with input from all coauthors.

*These authors contributed equally to this work.

‡These authors contributed equally to this work.

Competing interests: The authors declare no competing interests.

Data availability: Raw sequencing data will be available from ENA (accession no. PRJEB32566). An interactive data visualization application for the individuals used in this analysis is available at https://dcalderon.shinyapps.io/shiny_rome/.

SUPPLEMENTARY MATERIALS

science.sciencemag.org/content/366/6466/708/suppl/DC1

Figs. S1 to S30

Tables S1 to S28

References (37–195)

¹⁷Dipartimento di Studi Umanistici, Università degli Studi di Roma Tre, Rome, Italy. ¹⁸Soprintendenza Speciale Archeologia Belle Arti e Paesaggio di Roma, Rome, Italy. ¹⁹Servizio di Bioarcheologia, Museo delle Civiltà, Rome, Italy. ²⁰Christian and Medieval Archaeology, University of Rome Tor Vergata, Rome, Italy. ²¹Università della Tuscia, DISUCOM Dipartimento di Scienze Umanistiche, della Comunicazione e del Turismo, Viterbo, Italy. ²²Aix-Marseille University, Marseille, France. ²³Soprintendenza speciale Archeologia Belle arti e paesaggio di Roma, Rome, Italy. ²⁴University College Dublin, Dublin, Ireland. ²⁵Musei Vaticani, Reparto Antichità Greche e Romane, Vatican City. ²⁶Università L'Orientale Napoli, Naples, Italy. ²⁷Dipartimento di Archeologia, Università di Foggia, Foggia, Italy. ²⁸SABAP-LAZ Ministero dei Beni e delle Attività Culturali, Rome, Italy. ²⁹Department of Biology, Stanford University, Stanford, CA, USA.

Abstract

Ancient Rome was the capital of an empire of ~70 million inhabitants, but little is known about the genetics of ancient Romans. Here we present 127 genomes from 29 archaeological sites in and around Rome, spanning the past 12,000 years. We observe two major prehistoric ancestry transitions: one with the introduction of farming and another prior to the Iron Age. By the founding of Rome, the genetic composition of the region approximated that of modern Mediterranean populations. During the Imperial period, Rome's population received net immigration from the Near East, followed by an increase in genetic contributions from Europe. These ancestry shifts mirrored the geopolitical affiliations of Rome and were accompanied by marked interindividual diversity, reflecting gene flow from across the Mediterranean, Europe, and North Africa.

In the 8th century before the common era (BCE), Rome was one of many city-states on the Italian Peninsula. In less than 1000 years, it grew into the largest urban center of the ancient world (1–3). Rome controlled territory on three continents, spanning the entirety of the Mediterranean—or Mare Nostrum, “our sea,” as the Romans called it (1–3). As part of the Italian Peninsula, Rome occupies a distinctive geographic location. It is partially insulated by the Alps to the north, which formed a natural barrier to movement of languages, material cultures, and people (4, 5), and is also highly connected to regions around the Mediterranean Sea, particularly after Bronze Age advances in seafaring (2, 6).

Roman history has been extensively studied, but genetic studies of ancient Rome have been limited. To characterize the genetic composition of Rome's population throughout the trajectory of the empire, we assembled a time series of genetic data from 127 ancient individuals, spanning key events in Roman prehistory and history, allowing us to place genetic changes in the context of a rich archaeological and historical record.

Results

We generated whole-genome data for 127 ancient individuals from 29 archaeological sites in Rome and central Italy (Fig. 1 and table S1). Date estimates were obtained by direct radiocarbon dating ($n = 33$ individuals) and inference from archaeological context ($n = 94$) (tables S2 and S3). We powdered the cochlear portion of the petrous bone, extracted DNA,

and built partially uracil-DNA glycosylase (UDG)-treated libraries (7). Libraries were screened for endogenous DNA concentration, DNA damage patterns, and contamination. We performed whole-genome sequencing to a median depth of 1.05× genome-wide coverage (range 0.4 to 4.0×; table S2) and analyzed the data jointly with published ancient and modern genomes using principal component analysis (PCA), ADMIXTURE (8), *f*-statistics (9), and *qpAdm* admixture modeling (10) on pseudo-haploid genotypes; and ChromoPainter (11) on imputed diploid genotypes.

Individuals in this time series fall into three distinct genetic clusters according to chronology, as illustrated by PCA and ADMIXTURE (Fig. 2): (i) Mesolithic hunter-gatherers; (ii) early farmers (Neolithic and Copper Age individuals); and (iii) a broad historic cluster encompassing individuals from the Iron Age to the present. The historic individuals approximate modern Mediterranean and European populations in PCA space. However, there are highly variable ancestries among the historic individuals, both within and across time periods (Figs. 2 and 3).

The Mesolithic

The oldest genomes in our dataset are from three Mesolithic hunter-gatherers (10,000 to 7,000 BCE) from Grotta Continenza, a cave in the Apennine Mountains. In PCA, these individuals project close to Western hunter-gatherers (WHG) from elsewhere in Europe, including those from the Villabruna cave in northern Italy and from Grotta d’Oriente in Sicily (12–15) (fig. S17).

As reported previously for WHG groups (12,14), these individuals show particularly low heterozygosity, ~30% lower than that of early modern central Italians (7). After this period, we see a sharp increase in heterozygosity in the Neolithic Age and smaller increases afterwards, reaching modern levels by around 2000 years before present (fig. S6).

The Neolithic transition

The first major ancestry shift in the time series occurred between 7000 and 6000 BCE, coinciding with the transition to farming and introduction of domesticates including wheat, barley, pulses, sheep, and cattle into Italy (Fig. 2) (6,16).

Similar to early farmers from other parts of Europe, Neolithic individuals from central Italy project near Anatolian farmers in PCA (13,14,17–19) (Fig. 2A). However, ADMIXTURE reveals that, in addition to ancestry from northwestern Anatolia farmers, all of the Neolithic individuals that we studied carry a small amount of another component that is found at high levels in Neolithic Iranian farmers and Caucasus hunter-gatherers (CHG) (Fig. 2B and fig. S9). This contrasts with contemporaneous central European and Iberian populations who carry farmer ancestry predominantly from northwestern Anatolia (fig. S12). Furthermore, *qpAdm* modeling suggests that Neolithic Italian farmers can be modeled as a two-way mixture of ~5% local hunter-gatherer ancestry and ~95% ancestry of Neolithic farmers from central Anatolia or northern Greece (table S7), who also carry additional CHG (or Neolithic Iranian) ancestry (fig. S12) (14). These findings point to different or additional source populations involved in the Neolithic transition in Italy compared to central and western Europe.

During the late Neolithic and Copper Age, there is a small, gradual rebound of WHG ancestry (Fig. 2B and fig. S24), mirroring findings from ancient DNA studies of other European populations from these periods (10,13,18,20). This may reflect admixture with communities that had high levels of WHG ancestry persisting into the Neolithic, locally or in neighboring regions (tables S9 to S11).

The Iron Age and the origins of Rome

The second major ancestry shift occurred in the Bronze Age, between ~2900 and 900 BCE (Figs. 2 and 3, A and B, and tables S13 and S14). We cannot pinpoint the exact time of this shift because of a gap in our time series.

During this period, major technological developments increased the mobility of populations. The development of drafted chariots and wagons in the Near East and Pontic-Caspian Steppe enabled movement over land (21). Advances in sailing technologies facilitated easier and more frequent navigation across the Mediterranean (3, 6), enabling the expansion of Greek, Phoenician, and Punic colonies across the “Great Sea” and beyond in the late Bronze Age and Iron Age.

We collected data from 11 Iron Age individuals dating from 900 to 200 BCE (including the Republican period). This group shows a clear ancestry shift from the Copper Age, interpreted by ADMIXTURE as the addition of a Steppe-related ancestry component and an increase in the Neolithic Iranian component (Figs. 2B and 3B). Using *qpAdm*, we modeled the genetic shift by an introduction of ~30 to 40% ancestry from Bronze and Iron Age nomadic populations from the Pontic-Caspian Steppe (table S15), similar to many Bronze Age populations in Europe (10,13,14,19, 22). The presence of Steppe-related ancestry in Iron Age Italy could have happened through genetic exchange with intermediary populations (5,23). Additionally, multiple source populations could have contributed, simultaneously or subsequently, to the ancestry transition before Iron Age. By 900 BCE at the latest, the inhabitants of central Italy had begun to approximate the genetics of modern Mediterranean populations.

Although there is no direct historical or genetic information about the origins of Rome, archaeological evidence suggests that in the early Iron Age, it was a small city-state, among many culturally and politically similar Etruscan and Latin neighbors (24–26). Their contact with Greek and Phoenician-Punic colonies is evident in the incorporation of materials not available locally, such as ivory, amber, and ostrich eggshell, and design motifs such as lions, sphinxes, and palmettes, into Etruscan art and culture (3, 6).

The Iron Age individuals exhibit highly variable ancestries, hinting at multiple sources of migration into the region during this period (Figs. 2A and 3B). Although we were able to model eight of the 11 individuals as two-way mixtures of Copper Age central Italians and a Steppe-related population (~24 to 38%) using *qpAdm*, this model was rejected for the other three individuals ($p < 0.001$; table S16). Instead, two individuals from Latin sites (R437 and R850) can be modeled as a mixture between local people and an ancient Near Eastern population (best approximated by Bronze Age Armenian or Iron Age Anatolian; tables S17 and S18). An Etruscan individual (R475) carries significant African ancestry identified by *f*

statistics ($|Z\text{-score}| > 3$; fig. S23) and can be modeled with ~53% ancestry from Late Neolithic Moroccan (table S19). Together these results suggest substantial genetic heterogeneity within the Etruscan ($n = 3$ individuals) and Latin ($n = 6$) groups. However, using F -statistics, we did not find significant genetic differentiation between the Etruscans and Latins in allele sharing with any preceding or contemporaneous population ($|Z\text{-score}| < 2$), although the power to detect subtle genetic differentiation is limited by the small sample size.

In contrast to prehistoric individuals, the Iron Age individuals genetically resemble modern European and Mediterranean individuals, and display diverse ancestries as central Italy becomes increasingly connected to distant communities through new networks of trade, colonization, and conflict (3, 6).

Imperial Rome and the expanding empire

During the Republican (509 to 27 BCE) and Imperial (27 BCE to 300 CE) periods, Rome grew from a city-state on the Tiber river into an empire that spanned the entire Mediterranean and extended onto all three surrounding continents (3,6). Rome's overseas expansion began during the Punic Wars (264 to 146 BCE) against Carthage in present-day Tunisia (27). This growth continued for much of the next 300 years, reaching as far as Britannia, Morocco, Egypt, and Assyria. Rome itself had a population of over 1 million people, and it is estimated that the empire had a population of between 50 and 90 million (1). The empire facilitated the movement and interaction of people through trade networks, new road infrastructure, military campaigns, and slavery. Beyond the boundaries of the empire, Rome engaged in long-distance trade with northern Europe, sub-Saharan Africa, the Indian subcontinent, and across Asia (1–3,16). Although these contacts have been well documented, little is known about the genetic impacts.

During the Imperial period ($n = 48$ individuals), the most prominent trend is an ancestry shift toward the eastern Mediterranean and with very few individuals of primarily western European ancestry (Fig. 3C). The distribution of Imperial Romans in PCA largely overlaps with modern Mediterranean and Near Eastern populations, such as Greek, Maltese, Cypriot, and Syrian (Figs. 2A and 3C). This shift is accompanied by a further increase in the Neolithic Iranian component in ADMIXTURE (Fig. 2B) and is supported by F -statistics (tables S20 and S21): compared to Iron Age individuals, the Imperial population shares more alleles with early Bronze Age Jordanians (F_4 statistics $Z\text{-score} = 4.2$) and shows significant introgression signals in admixture f_3 for this population, as well as for Bronze Age Lebanese and Iron Age Iranians ($Z\text{-score} < -3.4$).

We attempted to fit the Imperial population as a simple two-way combination of the preceding Iron Age population and another population, either ancient or modern, using *qpAdm*. Some populations producing relatively better fits come from eastern Mediterranean regions such as Cyprus, Anatolia, and the Levant (table S22). However, none of the tested two-way models provides a good, robust fit to the data, suggesting that this was a complex mixture event, potentially including source populations that have not yet been identified or studied.

Although the data show a shift in the ancestry averaged across all Imperial individuals (referred to as “average ancestry” henceforth) toward eastern populations, the PCA results also suggest variation in ancestry within the population. To further characterize this, we assessed haplotype sharing using ChromoPainter (11), a method more sensitive than allele frequency-based approaches such as PCA. Specifically, we measured the genetic affinity between each ancient Italian individual and a set of modern Eurasian and North African populations by the total length of the haplotype segments shared between them (Fig. 4A) (7). We clustered ancient individuals by their relative haplotype sharing with modern populations and then labeled the resulting clusters by proximity to modern populations in PCA (Fig. 4B).

ChromoPainter analysis reveals diverse ancestries among Imperial individuals ($n = 48$), who fall into five distinct clusters (Fig. 4A). Notably, only 2 out of 48 Imperial-era individuals fall in the European cluster (C7) to which 8 out of 11 Iron Age individuals belong. Instead, two-thirds of Imperial individuals (31 out of 48) belong to two major clusters (C5 and C6) that overlap in PCA with central and eastern Mediterranean populations, such as those from southern and central Italy, Greece, Cyprus, and Malta (Fig. 4B). An additional quarter (13 out of 48) of the sampled Imperial Romans form a cluster (C4) defined by high amounts of haplotype sharing with Levantine and Near Eastern populations, whereas no pre-Imperial individuals appear in this cluster (Fig. 4AC). In PCA, some of the individuals in this cluster also project close to four contemporaneous individuals from Lebanon (240 to 630 CE) (fig. S18) (28). In addition, two individuals (R80 and R132) belong to a cluster featuring high haplotype sharing with North African populations (C4) and can be modeled with 30 to 50% North African ancestry in explicit modeling with *qpAdm* (table S28).

The shift in average ancestry and increase in complexity in the genetic composition follow the empire’s territorial expansion to encircle the entire Mediterranean (3). This connected Rome with people and cultures across the Mediterranean in unprecedented ways; however, our data show considerably more genetic influence from the eastern Mediterranean than elsewhere in the Empire.

Supporting this, there is evidence for the long-term settlement of people from the east in Rome. The most common language for inscriptions, after Latin, was Greek; other languages, such as Aramaic and Hebrew, were also used. Additionally, birthplaces recorded in burial inscriptions indicate that immigrants were commonly from the east (29). Temples and shrines to Greek, Phrygian, Syrian, and Egyptian gods were also common, and the earliest known synagogue in Europe was established in the Roman port-town of Ostia (3,16).

There is also well-documented evidence for connections between Rome and the west. For example, slaves were brought back to Rome from these regions following imperial expansions, such as Scipio Africanus’s victory over Carthage and Julius Caesar’s conquest of Gaul (1, 3,16). Rome also received large amounts of trade goods from the western Mediterranean, such as wine, garum, and olive oil from Gaul and Iberia; and grain, salt, and Tyrian purple dye from western North Africa (2, 3,16, 30). Unexpectedly, few Imperial individuals ($n = 2$) have strong genetic affinities to western Mediterranean populations, suggesting relatively limited immigration from the western provinces.

One possible explanation for the predominance of gene flow from the east into Rome is the higher population density in the eastern Mediterranean than the west. Historians have suggested that the large population size and the presence of megacities, such as Athens, Antioch, and Alexandria, may have driven a net flow of people from east to west during antiquity (31). In addition to direct immigration, eastern ancestry could also have arrived in Rome indirectly from Greek, Phoenician, and Punic diasporas that were established through colonies across the Mediterranean prior to Roman Imperial expansion (6,19, 23, 32).

As the majority of people and goods coming into Rome from the provinces arrived by boat, many of these would have docked at Rome's primary port—Portus Romae (33). The inhabitants of Portus were buried in the necropolis of Isola Sacra, where inscriptions indicate that many were engaged in commerce and business and frequently themselves descended from slaves (33). The individuals from Isola Sacra ($n = 9$) in this study typify both the Near Eastern genetic influence and interindividual diversity characteristic of the Imperial Roman population. Of the nine individuals from this site, four fall in the Near Eastern cluster (C4) in ChromoPainter, four in the eastern Mediterranean cluster (C5), and one (R37) in the European one (C7) (Fig. 4). All of these nine individuals have $\delta^{18}\text{O}$ isotope ratios compatible with having grown up in the local area (although alternative regions with similar isotopic profiles cannot be excluded), suggesting the long-term settlement of people with diverse ancestries in Rome (34).

Late Antiquity and the fall of Rome

Late Antiquity was characterized by deep demographic changes and political reorganization, including the split of the Roman Empire into eastern and western halves, the movement of the capital from Rome to Byzantium (later Constantinople), and the gradual dissolution of the Western Roman Empire (maps in Fig. 3, C and D) (1, 3).

The average ancestry of the Late Antique individuals ($n = 24$) shifts away from the Near East and toward modern central European populations in PCA (Fig. 3D). Formally, they can be modeled as a two-way mixture of the preceding Imperial individuals and 38 to 41% ancestry from a late Imperial period individual from Bavaria or modern Basque individuals (table S24). The precise identity of the source populations and the admixture fractions should not be interpreted literally, given the simplified admixture model assumed and the lack of data for most contemporaneous ancient populations (7). This ancestry shift is also reflected in ChromoPainter results by the drastic shrinkage of the Near Eastern cluster (C4), maintenance of the two Mediterranean clusters (C5 and C6), and marked expansion of the European cluster (C7) (Fig. 4C).

This shift may have arisen from reduced contacts with the eastern Mediterranean, increased gene flow from Europe, or both, facilitated by a drastic reduction in Rome's population in this period to less than 100,000 individuals, due to conflicts and epidemics (1, 3). After the move of the capital and the split of the Roman Empire, many of the networks of trade, grain supply, and governance that had previously flowed to and from Rome were rerouted to Constantinople (2). The reshaping of these networks would have affected the mobility of people, leading to weakened genetic affinity to the eastern Mediterranean. Additionally, large-scale movements of people from central Europe into Italy may have resulted from the

military campaigns of the Visigoths and Vandals in the 5th century CE and the long-term settlement of the Lombards in the region in the 6th and 7th centuries CE (1,3). Furthermore, the decline of Rome's population meant that even moderate amounts of immigration could have driven substantial changes in average ancestry.

The high interindividual heterogeneity observed in Imperial Rome continues into Late Antiquity (Figs. 3D and 4). Late Antique individuals are distributed across the eastern Mediterranean (C5), Mediterranean (C6), and European (C7) clusters in roughly equal proportions. Using f -statistics, we identified three outliers who are genetically distinct from others in the same period, including R104, who genetically resembles Sardinians, and R106 and R31, who overlap with modern Europeans in PCA (Fig. 3D). The persisting genetic diversity in Rome may have resulted from several sources, including prior trade, migration, slavery, and conquest during the Imperial period, as well as continued trade networks in the western Mediterranean and the movement of Visigoths, Vandals, and Lombards into Italy.

The genetic impact of Lombard settlement in northern Italy has been shown previously in individuals in Collegno during this time (35). Our data show that this impact potentially extended to Rome. One of our sites, Crypta Balbi, was originally built as a theater courtyard in the Imperial era and used for numerous subsequent purposes in Late Antiquity, including housing a workshop for Lombard-associated ornaments (such as belts, seals, and jewelry) and also as a burial space. Five of the seven individuals from this site are classified into the European cluster (C7) (Fig. 4 and fig. S17) and can be modeled as a mixture of the preceding Roman Imperial population and individuals from the Lombard-associated cemeteries in Collegno and Hungary (table S28).

The Medieval period and increasing ties to Europe

In the Medieval and early modern periods ($n = 28$ individuals), we observe an ancestry shift toward central and northern Europe in PCA (Fig. 3E), as well as a further increase in the European cluster (C7) and loss of the Near Eastern and eastern Mediterranean clusters (C4 and C5) in ChromoPainter (Fig. 4C). The Medieval population is roughly centered on modern-day central Italians (Fig. 3F). It can be modeled as a two-way combination of Rome's Late Antique population and a European donor population, with potential sources including many ancient and modern populations in central and northern Europe: Lombards from Hungary, Saxons from England, and Vikings from Sweden, among others (table S26).

This shift is consistent with the growing ties between Medieval Rome and mainland Europe. Rome was incorporated into the Holy Roman Empire (3), which spanned much of central and western Europe. The Normans expanded from northern France to a number of regions, including Sicily and the southern portion of the Italian Peninsula (and even sacked the city of Rome in 1084), where they established the Kingdom of Sicily (3, 36). Additionally, after the independence of Papal States, they remained closely (and sometimes contentiously) connected with the Holy Roman Empire, and Rome's role as a central place in the Roman Catholic Church brought people from across Europe, and eventually beyond, to Italy (3).

Summary

Our work outlines the genetic history of Rome and central Italy during the last 12,000 years. After two major prehistoric population turnovers—one with the introduction of farming and another prior to the Iron Age—individuals in central Italy began to genetically approximate modern Mediterranean populations. Throughout the past 3000 years, there were still pronounced ancestry shifts across time periods driven by genetic contributions from the Near East in the Imperial period, and later from Europe, mirroring changes in the political affiliations of Rome. Furthermore, within each time period, individuals exhibited highly diverse ancestries, including those from the Near East, Europe, and North Africa. These high levels of ancestry diversity began prior to the founding of Rome and continued through the rise and fall of the empire, demonstrating Rome's position as a genetic crossroads of peoples from Europe and the Mediterranean.

Supplementary Material

Refer to Web version on PubMed Central for supplementary material.

ACKNOWLEDGMENTS

We thank D. Pickel, A. van Oyen, J. Leidwanger, I. Hodder, W. Scheidel, N. Sinnott-Armstrong, D. Reich, and I. Mathieson for comments and discussions; L. Vitousek for assistance with Fig. 1; and the Chan Zuckerberg Biohub for sequencing.

Funding: This project was partially supported by National Science Foundation Graduate Research Fellowships (M.L.A. and D.J.C.); Stanford Interdisciplinary Graduate Fellowship and grants from the Stanford Archaeology Center and Stanford Anthropology Dept (H.M.M.); Howard Hughes Medical Institute (Z.G. and J.K.P.); and an MIUR grant (Project D15D18000410001) (G.M.).

REFERENCES AND NOTES

1. Harper K, *The Fate of Rome: Climate, Disease, and the End of an Empire* (Princeton Univ. Press, Princeton, 2017).
2. Horden P, Purcell N, *The Corrupting Sea: A Study of Mediterranean History* (Blackwell, 2000).
3. Abulafia D, *The Great Sea: A Human History of the Mediterranean* (Oxford Univ. Press, New York, 2011).
4. Petkova D, Novembre J, Stephens M, *Nat. Genet* 48, 94–100 (2016). [PubMed: 26642242]
5. Raveane A et al., *Sci. Adv* 5, w3492 (2019).
6. Broodbank C, *The Making of the Middle Sea: A History of the Mediterranean from the Beginning to the Emergence of the Classical World* (Oxford Univ. Press, 2013).
7. See supplementary materials.
8. Alexander DH, Novembre J, Lange K, *Genome Res.* 19, 1655–1664 (2009). [PubMed: 19648217]
9. Patterson N et al., *Genetics* 192, 1065–1093 (2012). [PubMed: 22960212]
10. Haak W et al., *Nature* 522, 207–211 (2015). [PubMed: 25731166]
11. Lawson DJ, Hellenthal G, Myers S, Falush D, *PLOS Genet.* 8, e1002453 (2012). [PubMed: 22291602]
12. Lazaridis I et al., *Nature* 513, 409–413 (2014). [PubMed: 25230663]
13. Mathieson I et al., *Nature* 528, 499–503 (2015). [PubMed: 26595274]
14. Mathieson I et al., *Nature* 555, 197–203 (2018). [PubMed: 29466330]
15. Fu Q et al., *Nature* 534, 200–205 (2016). [PubMed: 27135931]
16. Beard M, *SPQR: A History of Ancient Rome* (Liveright, New York, ed. 1, 2015).

17. Lazaridis I et al., *Nature* 548, 214–218 (2017). [PubMed: 28783727]
18. Hofmanova Z et al., *Proc. Natl. Acad. Sci. U.S.A* 113, 6886–6891 (2016). [PubMed: 27274049]
19. Olalde I et al., *Science* 363, 1230–1234 (2019). [PubMed: 30872528]
20. Fernandes DM et al., *Sci. Rep* 8, 14879 (2018). [PubMed: 30291256]
21. Anthony DW, *The Horse, the Wheel, and Language: How Bronze-Age Riders from the Eurasian Steppes Shaped the Modern World* (Princeton Univ. Press, Princeton, N.J., 2007).
22. Allentoft ME et al., *Nature* 522, 167–172 (2015). [PubMed: 26062507]
23. Fernandes DM et al., *The Arrival of Steppe and Iranian related ancestry in the islands of the western Mediterranean*. bioRxiv 584714 (2019).
24. Frascetti A, *Romolo il fondatore* (GLF editori Laterza, 2002).
25. Pallottino M, *Origini e storia primitiva di Roma: Texte imprimé* (Rusconi, 1993).
26. Grandazzi A, *The Foundation of Rome: Myth and History* (Cornell Univ. Press, 1997).
27. Miles R, *Carthage Must Be Destroyed: The Rise and Fall of an Ancient Mediterranean Civilization* (Allen Lane, London, 2010).
28. Haber M et al., *Am. J. Hum. Genet* 104, 977–984 (2019). [PubMed: 31006515]
29. Noy D, *Immigrants in Late Imperial Rome*, in *Ethnicity and Culture in Late Antiquity*, Mitchell S, Greatrex G, Ed. (David Brown Book Co., 2000).
30. Rickman GE, *Mem. Am. Acad. Rome* 36, 261–275 (1980).
31. Alcock S, in *The Cambridge Economic History of the Greco-Roman World*, Scheidel W, Morris I, Saller RP, Eds. (Cambridge Univ. Press, 2007).
32. Zalloua P et al., *Sci. Rep* 8, 17567 (2018). [PubMed: 30514893]
33. Garnsey P, *Osteodental biology of the people of Portus Romae (necropolis of Isola Sacra, 2nd–3rd cent. AD), enamel microstructure and developmental defects of the primary dentition Rome: National Prehistoric Ethnographic “L. Pigorini” Museum (CD-ROM)* (1999).
34. Prowse TL et al., *Am. J. Phys. Anthropol* 132, 510–519 (2007). [PubMed: 17205550]
35. Amorim CEG et al., *Nat. Commun* 9, 3547 (2018). [PubMed: 30206220]
36. Abulafia D, *The Two Italies: Economic Relations Between the Norman Kingdom of Sicily and the Northern Communes* (Cambridge Univ. Press, 2005).

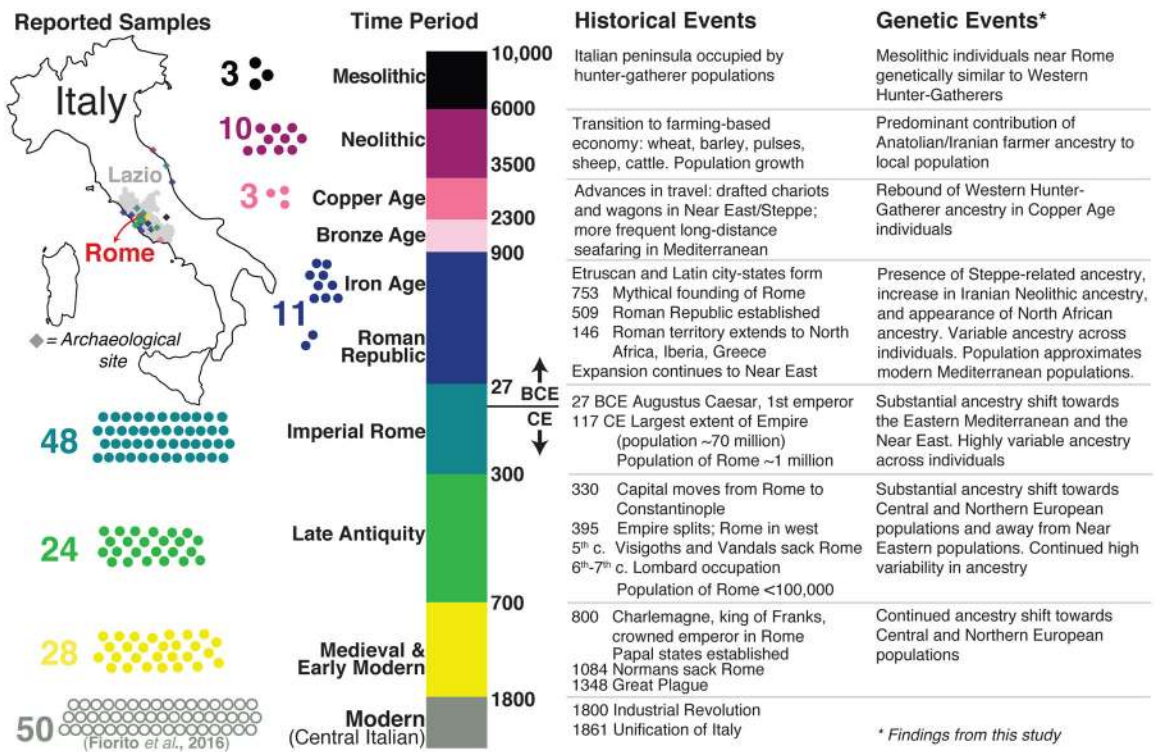


Fig. 1. Overview of study individuals, major events in Roman history, and key findings.

Time periods covered in this study are shown by color blocks, with reported samples represented by dots on the left side. A map of the sites from which individuals were sampled is shown in the top left. Present-day Rome, and its administrative province Lazio, are shown.

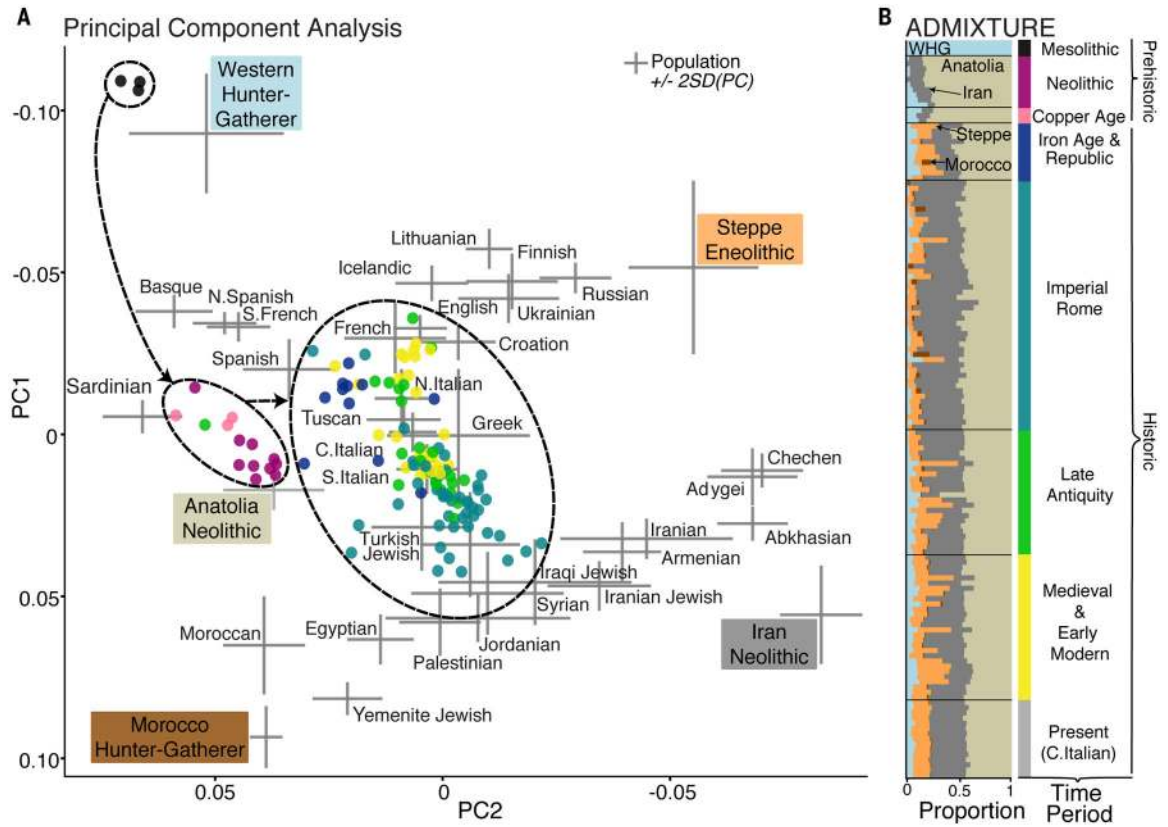


Fig. 2. Overview of the genetic structure of 127 ancient individuals from central Italy. (A) Individuals reported here (colored points) projected onto a principal component space defined by modern-day individuals. Crosses represent variation (± 2 SDs) of published ancient (black) and modern (gray) populations. Black circles and arrows highlight three major temporal clusters. The colored labels indicate five source populations used for supervised ADMIXTURE. (B) Supervised ADMIXTURE analysis performed with Western hunter-gatherer (WHG), Neolithic Anatolian, Neolithic Iranian, Eneolithic Steppe, and Morocco hunter-gatherer (Iberomausian) as the source populations ($k = 5$).

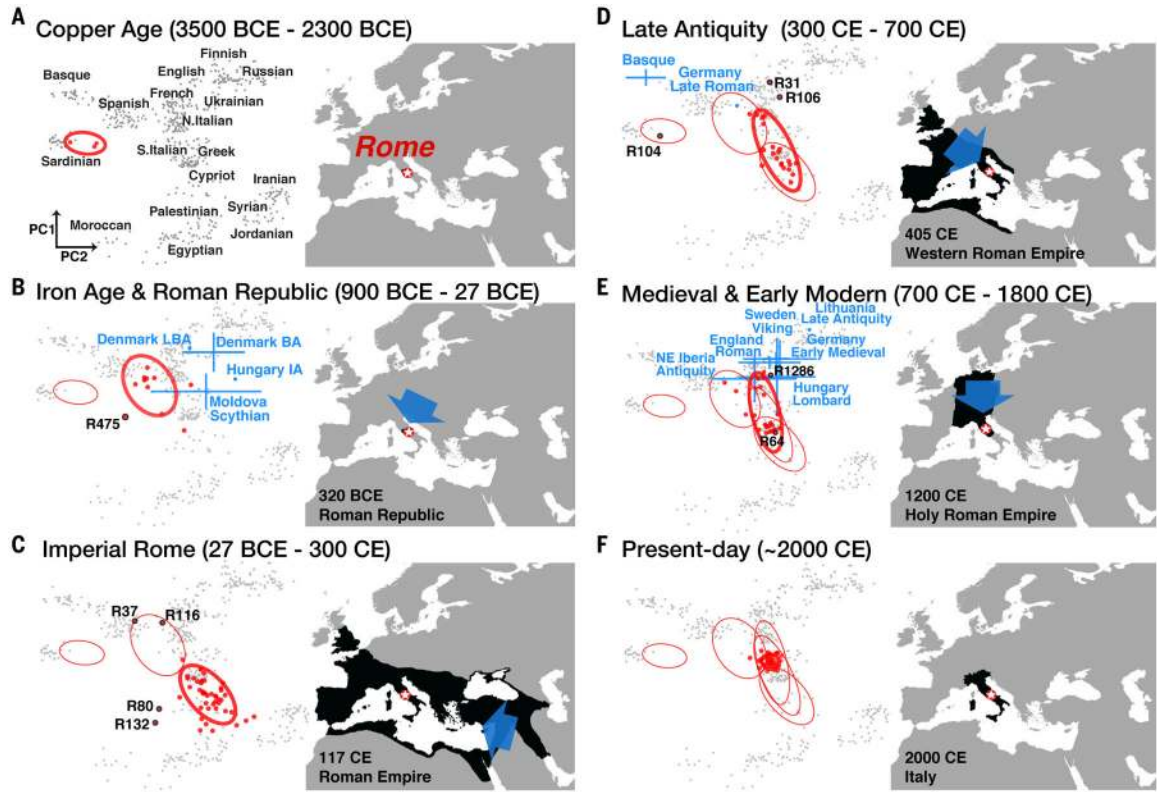


Fig. 3. Ancestry shifts of the Roman population during the historic era. (A to F) In each panel, the PCA (left) shows reported individuals (red points); a bold ellipse describes variation across individuals in this time period, whereas fainter ellipses are from preceding panels (multivariate t-distribution at a 0.80 confidence level). In blue are potential incoming sources identified by qpAdm modeling. The map (right) illustrates the territorial expanse of the political body encompassing Rome at the date specified at the bottom, with the blue arrow indicating the approximate direction of gene flow. No source provides an adequate fit for the Imperial Roman population (C). Individuals identified as outliers by an f_4 test are labeled with their sample IDs (table S27). Present-day populations are represented by gray points, with labels shown in (A).

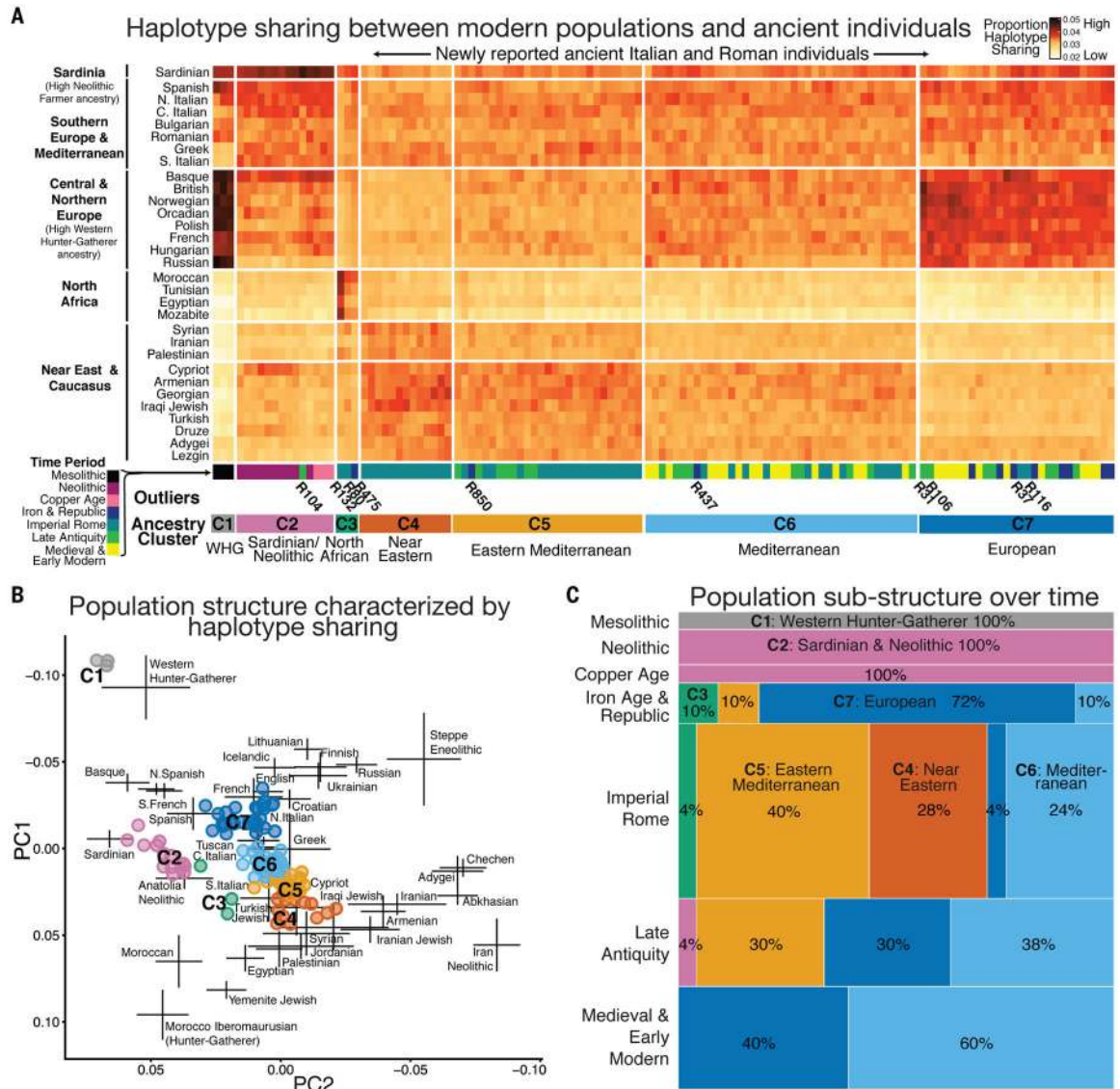


Fig. 4. Haplotype sharing between ancient Italian individuals and present-day population reveals fine population genetic structure.

(A) Total length of haplotype segments shared between present-day populations (rows) and reported study individuals (columns) (fig. S22). K-means clustering was performed on rows and columns. Individuals mentioned in the text are labeled with their sample IDs.

Annotations beneath the heatmap denote the time period for each individual and an identifier for the ancestry cluster. (B) PCA with study individuals (points) colored on the basis of their cluster membership in (A). (C) A mosaic plot showing the haplotype cluster membership [defined in (A)] for each time period (rows).